NASA Technical Memorandum 83436

Parametric Study of Flame Radiation Characteristics of a Tubular-Can Combustor

Francis M. Humenik, Russell W. Claus,
and Geralyn M. Neely
Lewis Research Center
Cleveland, Ohio

NASA

PARAMETRIC STUDY OF FLAME RADIATION CHARACTERISTICS
OF A TUBULAR-CAN COMBUSTOR

Francis M. Humenik
Russell W. Claus
and
Geralyn M. Neely
National Aeronautics and Space Administration
Lewis Research Center
Cleveland, Ohio 44135

ABSTRACT

A series of combustor tests were conducted with a tubular-car combustor to study flame radiation characteristics and effects with parametric variations in combustor operating conditions. Two alternate combustor assemblies using a different fuel nozzle were compared. Spectral and total radiation detectors were positioned at three stations along the length of the combustor can. Data were obtained for a range of pressures from 0.34 to 2.07 MPa (50 to 300 psia), inlet temperatures from 533 to 700K (500 to 800°F), for Jet A (13.9% hydrogen) and ERBS (12.9% hydrogen) fuels, and with fuel-air ratios nominally from 0.008 to 0.021. Spectral radiation data, total radiant heat flux data, and liner temperature data are presented to illustrate the flame radiation characteristics and effects in the primary, secondary, and tertiary combustion zones.

INTRODUCTION

Recent combustion experiments have emphasized the use of flame radiation measurements to determine effects of fuel quality variations on combustor emissions, flame temperature, and heat transfer characteristics (refs. 1, 2, 3). From analysis of the spectral flame radiance data, calculations of the flame temperature and soot concentration in each combustion zone yield some explanations for the effects observed (refs. 1, 4, 5). From analysis of total radiant heat flux data, some correlations with combustor liner temperatures have been demonstrated (ref. 2). Thus, combustor flame radiation measurements provide fundamental data that can be used to improve combustor liner thermal analysis and may help establish an analytical heat transfer model. These analytical efforts may yield improved liner durability in future designs by prescribing optimum adjustments to cooling airflow distribution. Also, liner development costs may be reduced by minimizing design iterations.

In order to expand the fundamental flame radiation data base, the series of combustor tests initiated with reference 1 were continued in order to provide a more complete mapping and parametric investigation of combustor operating variables on flame radiation. Three window-stations and three transducer-stations along the length of the combustor housing assembly provided access for spectral and total radiation sensors respectively. Thus, the flame radiation characteristics and effects in the three combustion zones could be compared.

The primary purpose of this report is to present an overall general description of the variation in spectral and total flame radiation characteristics in each combustion zone with variations in combustor operating conditions, reduction in fuel hydrogen content, and choice of fuel nozzle.

Data were obtained for a range of pressures from 0.34 to 2.07 MPa (50 to 300 psia), inlet temperatures from 533 to 700K (500 to 800°F) and for Jet A (13.9% hydrogen) and a research test fuel, ERBS (12.9% hydrogen, ref. 6). A single spectral radiance sensing system and three total radiant heat flux transducers provided measurements at the three locations along the length of the combustor can. Data from these sensors along with selected liner thermocouple data are presented to illustrate the flame radiation characteristics and effects in the primary, secondary, and tertiary combustion zones.

APPARATUS AND PROCEDURE

The flame radiation experiments were conducted with a single JT8D tubular can combustor installed in a standard pipe section (25.4 cm, 10 inch, nominal diameter) modified to be a test housing assembly as shown in the schematic illustration of figure 1. Combustor inlet instrumentation consisted of two inlet static pressures and a five point inlet thermocouple rake (Chromel-Alumel) located in the inlet plenum section. The com-

bustor exit instrumentation (see figure 1) consisted of a set of eight-five point thermocouple rakes (platinum - 13 percent rhodium/ platinum) for monitoring the exit temperature pattern and a set of four gas sample probes for routine exhaust gas analysis. Liner metal temperatures were measured with 24 thermocouples (Chromel-Alumel) of which 4 were located on the dome and the others divided along opposite sides of the combustor can to give 2 separate thermocouples on the outside of each cooling louver.

The flame radiation instrumentation consisted of three separate radiant heat flux transducers installed for continuous measurements at three stations along the combustor housing and a single spectral radiation detector unit positioned in line with one of the three window ports as illustrated in figure 2. The three radiant heat flux transducers were a Gardon-type gauge that senses the radial transfer of heat to a sink by use of a differential thermoelectric circuit. Each transducer was water-cooled and required a continuous nitrogen purge to sweep the sensor tip. The stem of the transducer extended to the inner surface of the combustor liner through an existing air entry hole or a specially added clearance hole. The measurement locations nominally corresponded to primary (#1), secondary (#2), and tertiary (#3) combustion zones. Thus, a reading of total radiant heat flux in each combustion zone was obtained with each spectral scan of the flame radiance at a selected window port.

The spectral radiation system components included an optical sensing head unit, a programmable controller, and a printer as shown in figure 3. The sensing head consisted of an optical radiation telescope system, a variable spectral filter system, and an indium antimonide radiation detector which required high pressure gaseous nitrogen

for cooling. The programmable controller provided a choice of step-scanning cycle for sensing at the desired wavelength increments. Further details and description of the spectral radiometer apparatus are given in reference 1. The location of the window ports for spectral measurements and the location of the three total radiant heat flux transducers are included with the photographs of the JT8D tubular can combustor in figure 4.

The arrangement of the apparatus in the test facility is shown in the photograph of figure 5. The exit instrumentation rakes and gas sample probes are on the left. The flow direction is right to left. The spectral viewing ports contained sapphire windows whose transmittance bandwidth and high temperature capability are suited to this application. For safety reasons, local focusing of the spectral detector optics and optimizing the output signal was conducted only at low pressure (0.34 MPa, 50 psia). Spectral data scanning and recording was initiated from an adjacent control room.

Two candidate fuel nozzles, FN#1 and FN#2, were selected for comparison in this test program. FN#1 was a standard type fuel nozzle for a conventional JT8D assembly configuration; FN#2 was a commercial substitute offered for experimental comparison. Both fuel nozzles, FN#1 and FN#2, were the dual orifice pressure atomizing type. From flow calibrations of each fuel nozzle, FN#2 produced a higher flow rate than FN#1 (by about 10-15%) at representative primary and secondary test pressures but no other significant differences were apparent. Testing was initiated with fuel nozzle FN#1 to obtain a representative set of data; then with fuel nozzle FN#2, a more complete data set was obtained which included tests with both Jet A (13.9% hydrogen) and ERBS (12.9% hydrogen) fuels.
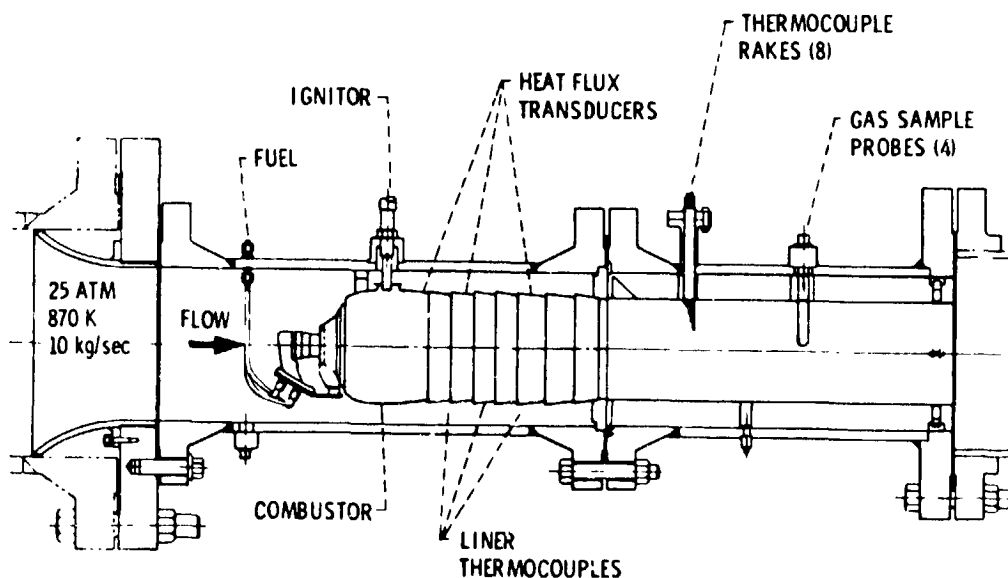

Figure 1. - Schematic of tubular combustor installation. Nominal flow capabilities of test facility: inlet pressure, 25 atm; inlet air temperature, 870 K; inlet airflow rate, 10 kg/sec.

2

TOTAL RADIOMETERS

ZONE 1
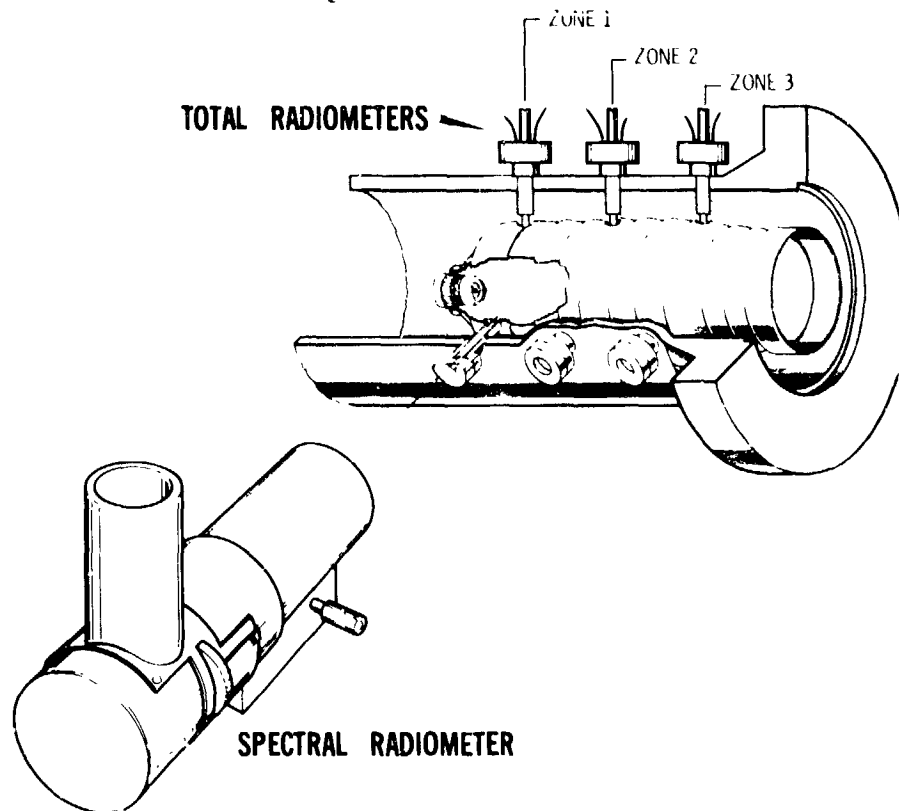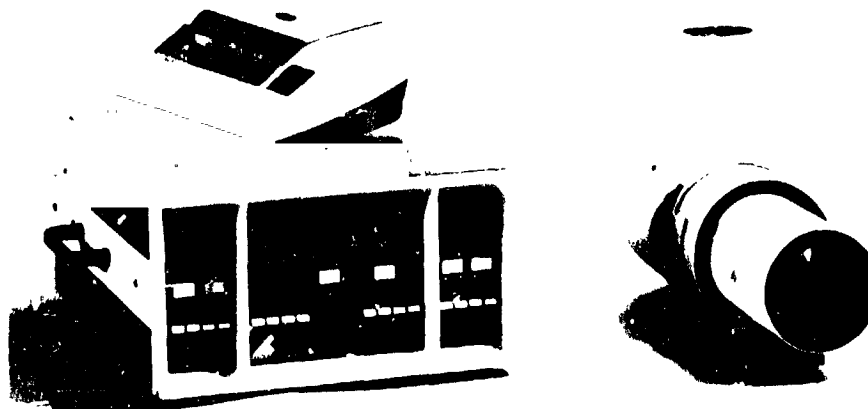ZONE 2
ZONE 3

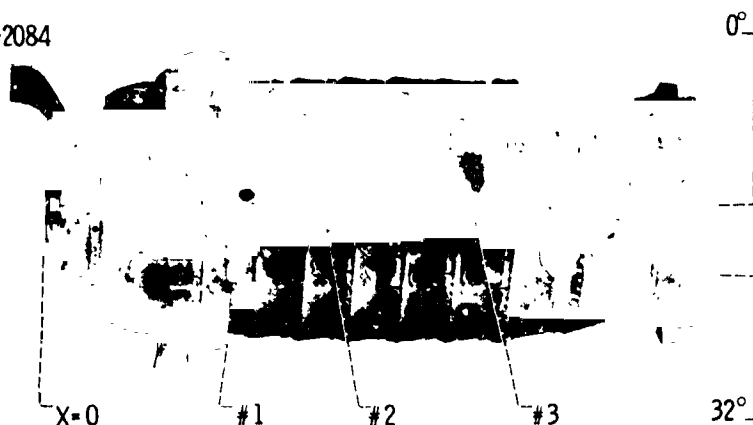SPECTRAL RADIOMETER

Figure 2. - Assembly of tubular combustor for flame radiation studies.

C 80 0537

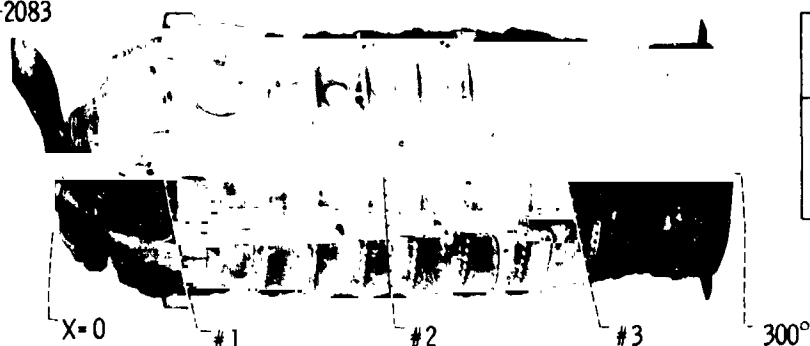Figure 3. Spectral radiometer system components: programmable controller with printer, and sensing head.

C-83-2084

RADIANT HEAT FLUX

ZONE	X, LOCATION		θ, LOC.
	cm	in.	deg
1	12.7	5.0	32
2	18.5	7.3	0
3	28.7	11.3	0

C-83-2083

SPECTRAL RADIANCE

ZONE	X, LOCATION		θ, LOC.
	cm	in.	deg
1	7.4	2.9	300
2	22.1	8.7	300
3	34.0	13.4	300

Figure 4. - Photographs of tubular-can combustor with flame radiation zone locations.
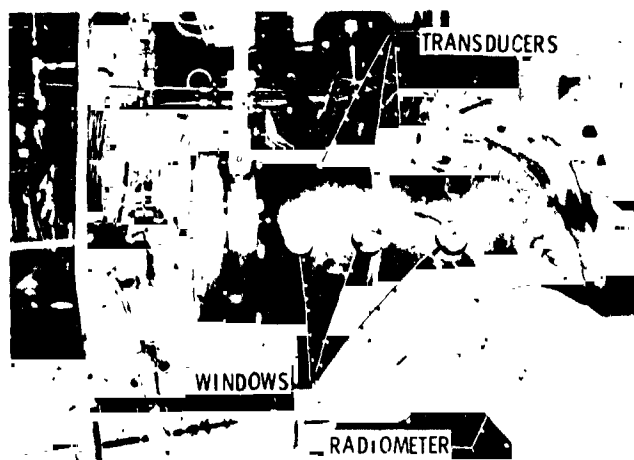

Figure 5. - Photograph of JT8D combustor housing assembly during experiments. Installation of radiant heat flux transducers, location of window-stations and spectral radiometer sensing head are shown.

4

Test conditions (see Table I) were selected to cover the normal range of combustor operation while maintaining a constant mass flow parameter for the parametric variations. Test conditions include combustor pressures of 0.34 MPa (50 psia), 0.69 MPa (100 psia), 1.38 MPa (200 psia), and 2.07 MPa (300 psia); combustor inlet temperatures of 533K (500°F), 616K (650°F) and 700K (800°F); with fuel-air ratios nominally from 0.008 to 0.021.

Test fuels (see Table II) included the conventional Jet A and the experimental ERBS fuel (ref. 6). Many recent combustion experiments have included tests with ERBS fuel because it is representative of a possible future fuel that has potential for use if another fuel crisis occurs or fuel supplies are disrupted. The data obtained with this fuel indicate combustion performance trends with reductions in fuel hydrogen content.

Measurement of airflow rates were obtained from a conventional ASME orifice station; measurement of fuel flow rates were obtained from conventional turbine type flowmeters. The NASA Lewis ESCORT automatic data acquisition system provided on-line instantaneous monitoring of data with formal data recording and batch processing using the laboratory IBM 370/3033 system.

TABLE I. - TEST CONDITIONS

Combustor pressure		Combustor inlet temperature		Airflow rate	
MPa	psia	K	°F	kg/sec	lb/sec
0.34	50	533	500	1.69	3.72
.69	100			3.37	7.44
1.38	200	↓	↓	6.75	14.88
2.07	300			10.12	22.32
0.69	100	616	650	3.14	6.92
1.38	200	616	650	6.28	13.84
2.07	300	616	650	9.42	20.76
0.69	100	700	800	2.95	6.50
2.07	300	700	800	8.84	19.50

TABLE II. - FUEL CHARACTERISTICS

Specifications	Jet-A	ERBS
ASTM distillation, K:		
Initial boiling point	411	435
10 percent evaporated	451	461
50 percent evaporated	479	488
90 percent evaporated	517	552
Final boiling point	531	601
Specific gravity at 289 K	0.8142	0.8381
Freezing point, K	226	244
Viscosity at 250 K, m^2/sec	5×10^{-6}	7.2×10^{-6}
Net heat of combustion, J/g	43 304	42 200
Hydrogen, percent by weight	13.9	12.9
Aromatics, percent by volume	17.2	28.8
Sulfur (total), percent by weight	0.020	0.065

RESULTS AND DISCUSSION

Fundamental flame radiation data were obtained with an experimental tubular can combustor configuration to determine variations in flame radiance characteristics for a range of parametric test conditions. Data are presented in figures 6 to 9 to illustrate some fundamental flame radiation characteristics which are useful for comparing performance trends, examining correlations, and explaining variations in each combustion zone. Specific results discussed are as follows:

1) comparison of two candidate fuel nozzles, figure 6;

2) spectral flame radiance variation, figure 7;

3) total radiant heat flux variation, figure 8;

4) comparison of radiant heat flux with liner temperature, figure 9.

Comparison of Fuel Nozzles

The variations in radiant heat flux distribution with variations in fuel-air ratio produced by fuel nozzles FN#1 and FN#2 with Jet A fuel are shown in figure 6. These data are grouped to compare the results in each combustor zone at the low combustor pressure of 0.69 MPa (100 psia) with the high combustor pressure of 2.07 MPa (300 psia). In general, significantly different rates of radiant heat flux variation are apparent in each zone along with an overall increase in radiant heat flux levels with combustor pressure increase.

The specific characteristics for combustion zone #1 (primary, see figure 6(a) and (b) only) show that FN#2 produced higher radiant heat flux than FN#1 at both the low and high combustor pressure levels for fuel-air ratios from 0.012 and greater. Since soot is a major contributor to total flame radiation, increased levels of radiant heat flux are usually an indicator of higher soot concentrations. However, other data (higher local liner temperatures and higher exhaust NO_x levels) indicate that primary zone flame temperatures may also have been higher with FN#2. For instance, at the low pressure condition with f/a = 0.018, local liner temperatures were 50K (89°F) higher in this zone with FN#2 whereas at the high pressure condition with f/a = 0.016, local liner temperatures were 34K (60°F) higher with FN#2. Similarly, exhaust NO_x levels were 12 ppm higher (82 ppm vs 94 ppm) at the low pressure condition (f/a = 0.018) with FN#2 and 45 ppm higher (86 ppm vs 131 ppm) at the high pressure condition (f/a = 0.016) with FN#2. These data are indicators that FN#2 produced higher flame temperatures resulting in substantially increased NO_x levels and higher local liner temperatures. Thus, a combination of higher flame temperatures and increased soot concentration may have produced the higher radiant heat flux in this zone with FN#2.

The characteristics in combustion zone #2 (secondary, see figure 6(c) and (d) only) show rapidly changing combustion reaction conditions occurring in this zone with increase in fuel-air ratio. With FN#2, there was a very steep increase in radiant heat flux at the high combustor pressure condition ranging from 16 W/cm² (f/a = 0.0089) to a peak of 80 W/cm² (f/a = 0.0159). With FN#1, the peak radiant heat flux level was 77 W/cm² (f/a = 0.0130). Thus, at the high pres-

5

sure condition, relatively high radiant heat flux levels are evident in the secondary zone with either fuel nozzle.

The characteristics in combustion zone #3 (tertiary, see figure 6 (e) and (f) only), show that FN#1 yielded higher radiant heat flux than FN#2 at both low and high combustor pressure levels. In this zone, combustor temperatures have been reduced, combustion reactions are completed, and therefore, the radiant heat flux levels are attributed solely to soot concentration. Thus, with the substantial difference in radiant heat flux levels between the two fuel nozzles, it is evident that FN#1 results in higher exhaust smoke levels than FN#2. Since FN#2 produced much higher exhaust NO_x levels, a tradeoff between exhaust smoke and exhaust NO_x was obtained by the choice of fuel nozzle alone.

In summary, the substitute experimental fuel nozzle, FN#2, produced a significant re-distribution of total radiant heat flux between combustion zones. It is also apparent that radiant heat flux levels in each zone increased with increase in combustor pressure. Finally, the combustor assembly with FN#2 produced less exhaust smoke than FN#1, but higher exhaust NO_x levels. The combustor assembly with FN#2 was utilized for all subsequent testing.

Spectral Flame Radiance Variation

The variations in spectral flame radiance for nominal fuel/air ratios of 0.016 obtained with fuel nozzle FN#2, and with Jet A and ERBS fuels are shown in figure 7. Data at 0.34 MPa (50 psia) and 0.69 MPa (100 psia) are prese 'ed in order to focus on the comparison of differences between the two fuels. Data at higher pressures up to 2.^7 MPa (300 psia) were also obtained but did not reveal any significant fuel differences.

In combustion zone #1 (primary, see fig. 7(a) and (b)), spectral flame radiance levels at a nominal reference wavelength near 1.5 μm and combustor pressure of 0.34 MPa (50 psia) was about 1.3 W/(cm^2 sr μm) with Jet A fuel and increased to about 2.7 W/(cm^2 sr μm) with ERBS fuel. With combustor pressure of 0.69 MPa (100 psia), spectral flame radiance levels increased substantially to 4.2 W/(cm^2 sr μm) with Jet A fuel and to 4.5 W/(cm^2 sr μm) with ERBS fuel. The peaks at about 4.5 μm wavelength are due to CO_2 band radiance and are an indicator of flame temperature (ref. 1). Comparing the peaks indicates only slightly reduced flame temperature with combustor pressure increase but substantial flame radiance increase which is thus attributed to substantial increase in soot concentration. The increase in flame radiance with ERBS fuel (12.9% hydrogen) was most evident at the low combustor pressure and tends to be less distinct at high combustor pressures.

In combustion zone #2 (secondary, see figure 7(c) and (d)), spectral flame radiance levels at 1.5 μm wavelength and combustor pressure of 0.34 MPa (50 psia) was about 1.2 W/(cm^2 sr μm) with Jet A fuel and increased to about 2.4 W/(cm^2 sr μm) with ERBS fuel. With combustor pressure of 0.69 MPa (100 psia), spectral flame radiance levels increased substantially to about 5.7 W/(cm^2 sr μm) with both Jet A and ERBS fuels. The similarity in CO_2 band radiance peaks at 4.5 μm wavelength indicates very little difference in flame temperature at both combustor pressures

and with either fuel. Thus, only a small increase in soot concentration was evident at the lower combustor pressure with the ERBS fuel. The peaks at 2.7 μm wavelength are the contribution to the flame radiance due to water vapor which are most evident at low combustor pressures.

In combustion zone #3 (tertiary, see figure 7 (e, and (f)), spectral flame radiance levels were generally below 0.6 W/(cm^2 sr μm) with both combustor pressures and with both fuels. The CO_2 band radiance peaks are very similar and indicate the lowering of combustor temperature in this zone. It thus appears that soot concentration levels are practically identical with either fuel and greatly reduced compared to zones #1 and #2.

Thus, despite higher soot levels produced in the primary zone with ERBS fuel, the additional soot was burned up before it reached the combustor exit. This indicates that with either fuel there was no discernible difference in exhaust smoke levels.

Total Radiant Heat Flux Variation

The variations in total radiant heat flux with increase in combustor pressure for each combustion zone are shown in figure 8. These data were obtained with FN#2 for a nominal fuel-air ratio of 0.016, inlet temperatures of 533K (500°F) and 616K (650°F), with Jet A and ERBS fuels. There is a fast rate of increase in radiant heat flux in combustion zones #1 and #2 at the low combustor pressure levels and a slow rate of increase in radiant heat flux at the high combustor pressure levels. This generally corresponds to the expected increase in flame emissivity with increase in combustor pressure. Combustor zones #1 (primary) and #2 (secondary) produced very similar levels of radiant heat flux ranging from about 16 W/cm^2 at low combustor pressures to about 78 W/cm^2 at a combustor pressure of 2.07 MPa (300 psia) with Jet A fuel (see figure 8(a)); whereas, combustor zone #3 (tertiary) was much lower and ranged only from about 7 to 29 W/cm^2 for this range of test conditions. There was a small increase of up to 10 W/cm^2 in radiant heat flux intensity in each zone with ERBS fuel compared to Jet A fuel. The effect of increasing the combustor inlet temperature by 82K (150°F) did not produce a notable variation in the intensity of the radiant heat flux (see figure 8 (a) and (b)).

Comparison of Radiant Heat Flux with Liner Temperatures

The total radiant heat flux data in each combustion zone for two combustor pressures of 0.69 MPa (100 psia) and 2.07 MPa (300 psia); nominal f.el-air ratio of 0.016; for Jet A and ERBS fuels are shown in figure 9(a) for an inlet temperature of 533K (500°F) and in figure 9(b) for an inlet temperature of 700K (800°F). The corresponding local liner temperature data are shown in figure 9(c) and (d) respectively. These data illustrate that although the radiant heat flux increased as expected with combustor pressure increase, the liner temperatures for a combustor pressure of 2.07 MPa (300 psia) were substantially lower than those for a combustor pressure of 0.69 MPa (100 psia). This is attributed to a large increase in convective cooling at high pressures sufficient to offset the increased flame radiation and still reduce liner temperatures. There also was an increase in radiant heat flux and liner temperatures

with the increase in combustor inlet temperature from 533K (500°F) to 700K (800°F). This is an indicator that flame temperatures increased proportionately and that the film cooling effectiveness is also reduced with the higher inlet temperature condition. The ERBS fuel data consistently indicated an additional increase in radiant heat flux and liner temperatures in each combustion zone compared to the Jet A fuel data. A large increase of 33K (59°F) in local liner temperature with the ERBS fuel was especially evident in combustion zone #2 with combustor pressure of 0.69 MPa (100 psia) and combustor inlet temperature of 533K (500°F). The highest radiant heat flux occurred in combustion zone #1 (primary) with a combustor pressure of 2.07 MPa (300 psia) and combustor inlet temperature of 700K (800°F); whereas, the highest differential liner temperatures also occurred in combustion zone #1 but at the lower combustor pressure of 0.69 MPa (100 psia) with combustor inlet temperature of 700K (800°F).

SUMMARY OF RESULTS

Spectral flame radiance characteristics and total radiant heat flux measurements were obtained with a tubular can combustor for a range of pressures from 0.34 to 2.07 MPa (50 to 300 psia), inlet air temperatures from 533 to 700K (500 to 800°F), and for Jet A and ERBS (12.9% hydrogen) fuels.

A comparison of two fuel nozzles over a range of fuel-air ratios from 0.0087 to 0.0212 was illustrated with Jet A fuel. A substitute experimental fuel nozzle produced a re-distribution of total radiant heat flux between combustion zones, substantially higher total radiant heat flux levels in the primary zone, a steep increase in secondary zone heat flux from 16 W/cm^2 (f/a, 0.0089) to a peak of 80 W/cm^2 (f/a, 0.0159) with a combustor pressure of 2.07 MPa (300 psia), and lower total radiant heat flux levels in the tertiary zone.

The other significant flame radiation characteristics and effects for the tubular-can combustor with the substitute fuel nozzle are as follows:

1. For a fuel-air ratio of 0.016, and inlet air temperature of 533K (500°F), the spectral flame radiance (nominal wavelength near 1.5 µm) substantially increased from a level of about 1.3 to 4.2 W/(cm^2 sr µm) in the primary zone, from 1.2 to 5.7 W/(cm^2 sr µm) in the secondary zone, and from 0.15 to 0.6 W/(cm^2 sr µm) in the tertiary zone with a combustor pressure increase from 0.34 MPa (50 psia) to 0.69 MPa (100 psia) using Jet A fuel.

2. For a fuel-air ratio of 0.016, and inlet air temperature of 533K (500°F), the total radiant heat flux substantially increased from a level of about 16 W/cm^2 to 66 W/cm^2 in the primary zone, from 16 to 78 W/cm^2 in the secondary zone, and from 7 to 29 W/cm^2 in the tertiary zone with a combustor pressure increase from 0.34 MPa (50 psia) to 2.07 MPa (300 psia) using Jet A fuel.

3. A comparison of total radiant heat flux variation and differential local liner temperature variation by combustion zone for a fuel-air ratio of 0.016 revealed that with a combustor inlet air temperature of 700 K (800°F), the highest radiant heat flux occurs in the primary zone with a combustor pressure of 2.07 MPa (300 psia); whereas, the highest differential liner temperatures occur with a combustor pressure of 0.69 MPa (100 psia), and also in the primary zone.

4. There was an increase in local liner temperatures with ERBS fuel which ranged up to 33K (59°F) higher than those obtained with Jet A fuel in combustion zone #2 at low power conditions of 0.69 MPa (100 psia), 533K (500°F), f/a = 0.016.

CONCLUDING REMARKS

Flame radiation data are a necessary input to the fundamental data base required for advanced liner thermal analysis and to establish an analytical heat transfer model. The data which have been presented indicate the general flame radiation characteristics and effects produced with variations in operating conditions and choice of fuel nozzle. More detailed heat transfer analysis and other auxiliary calculations using the data from this test program are continuing and undergoing evaluation. The preliminary interpretations of this data are based on the previous experiments which are referenced as applied to this data set.

REFERENCES

1. Claus, Russell W.: Spectral Flame Radiance from a Tubular-Can Combustor. NASA TP-1722, 1981.

2. Kuznar, R. J.; Tobery, E. W.; and Cohn, A.: Combustor Flame Radiation and Wall Temperatures for #2 Distillate and a Coal Derived Liquid Fuel. ASME Paper No. 82-GT-208.

3. Najjar, Y. S. H.; and Goodger, E. M.: Radiation and Smoke from the Gas Turbine Combustor Using Heavy Fuels. ASME Paper No. 81-HT-21.

4. Norgren, Carl. T.: Determination of Primary-Zone Smoke Concentrations from Spectral Radiance Measurements in Gas Turbine Combustors. NASA TN D-6410, 1971.

5. Norgren, Carl T.; and Ingebo, Robert D.: Spectral Radiance Measurements and Calculated Soot Concentrations Along the Length of an Experimental Combustor. NASA TM X-3394, 1976.

6. Seng, Gary T.: Characterization of an Experimental Referee Broadened-Specification (ERBS) Aviation Turbine Fuel and ERBS Fuel Blends. NASA TM-82883, August 1982.
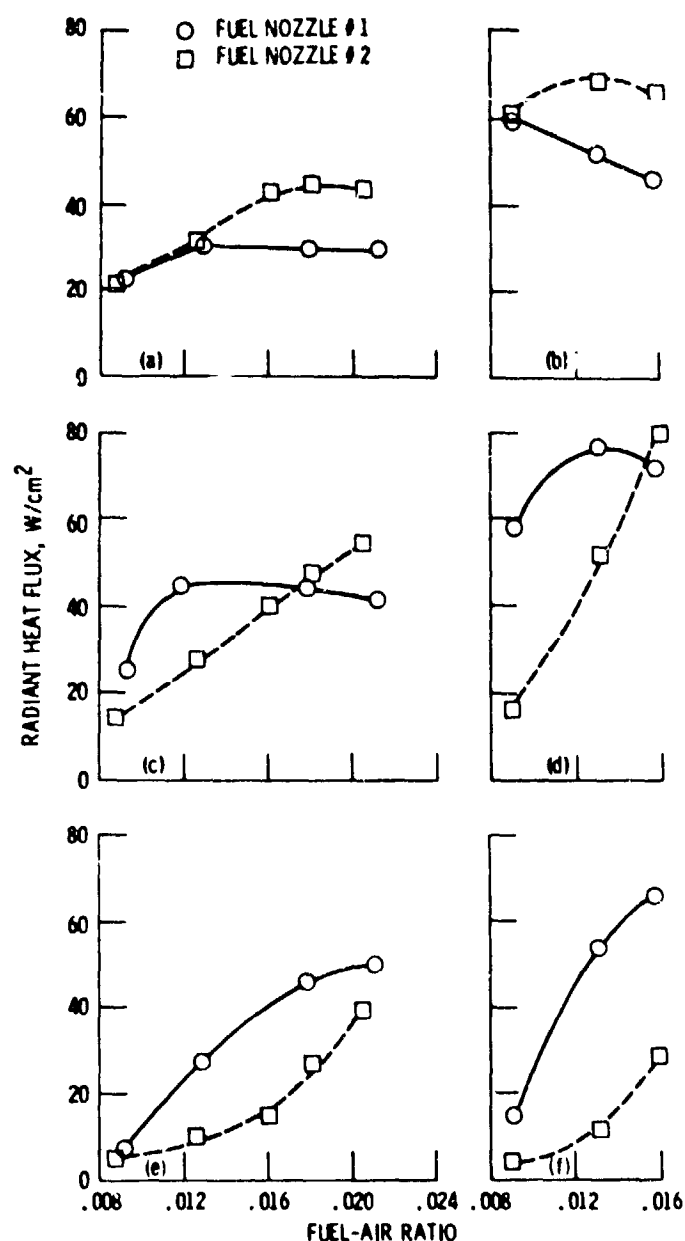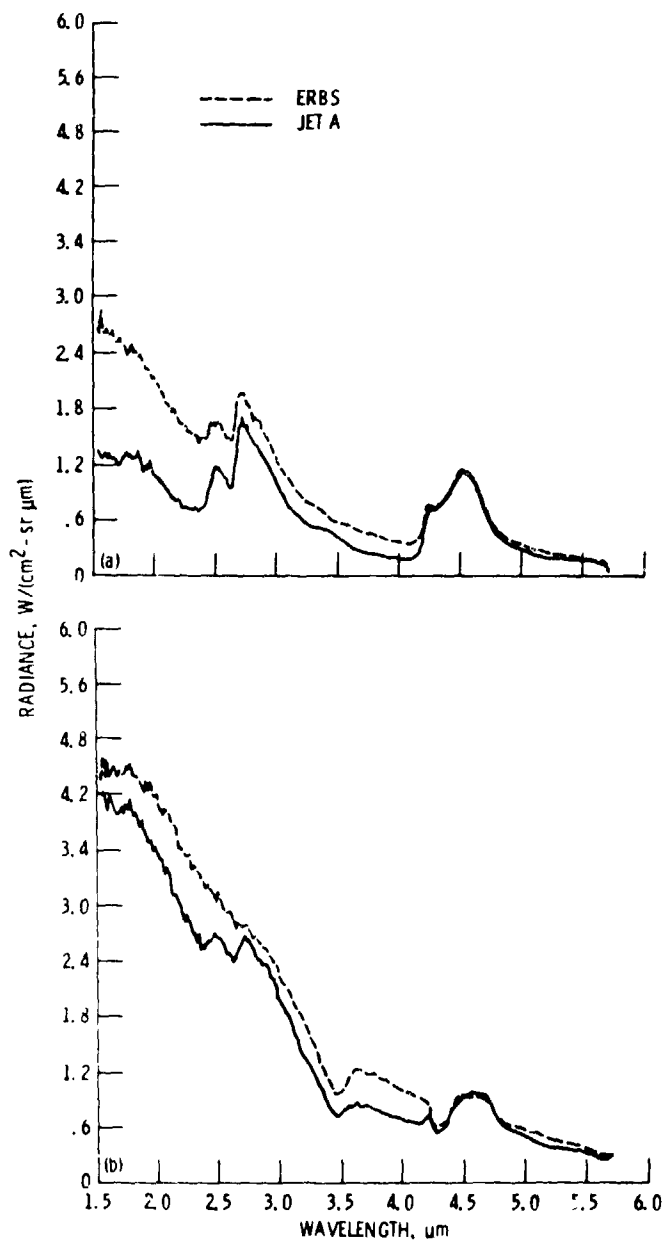
(a) Zone #1 (primary); combustor pressure, 0.69 MPa (100 psia).

(b) Zone #1 (primary); combustor pressure, 2.07 MPa (300 psia).

(c) Zone #2 (secondary); combustor pressure, 0.69 MPa (100 psia).

(d) Zone #2 (secondary); combustor pressure, 2.07 MPa (300 psia).

(e) Zone #3 (tertiary); combustor pressure, 0.69 MPa (100 psia).

(f) Zone #3 (tertiary); combustor pressure, 2.07 MPa (300 psia).

Figure 6. - Comparison of standard (FN-1) and substitute (FN-2) fuel nozzles: variation in total radiant heat flux with variation in fuel-air ratio; Jet A fuel; inlet air temperature, 533 K (500° F).

(a) Zone #1 (primary); combustor pressure, 0.34 MPa (50 psia).
(b) Zone #1 (primary); combustor pressure, 0.69 MPa (100 psia).

Figure 7. - Variation in spectral flame radiance with spectral wavelength; fuel air ratio, 0.016; Jet A and ERBS fuels; inlet air temperature, 533 K (500° F); fuel nozzle, FN #2.
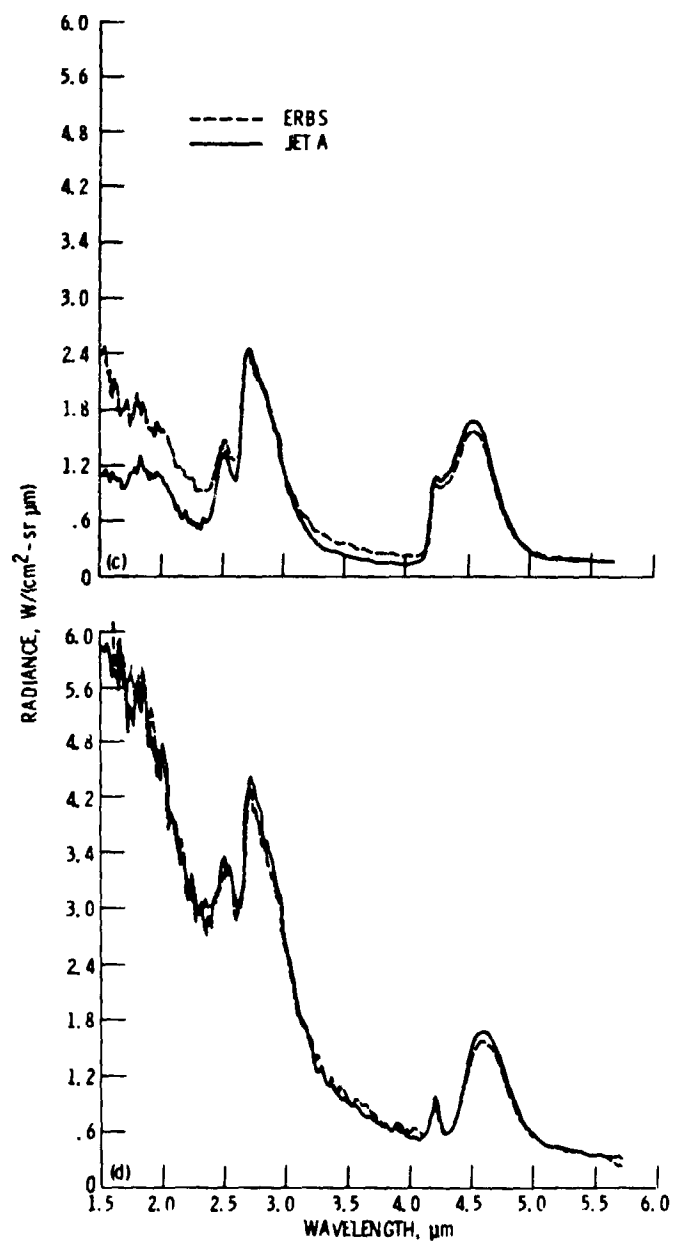
(c) Zone #_ (secondary); combustor pressure, 0.34 MPa (50 psia).
(d) Zone #2 (secondary); combustor pressure, 0.69 MPa (100 psia).

Figure 7. - Continued.

9

(e) Zone #3 (tertiary); combustor pressure, 0.34 MPa (50 psia).

(f) Zone #3 (tertiary); combustor pressure, 0.69 MPa (100 psia).

Figure 7. - Concluded.

(a) Inlet air temperature, 533 K (500° F).

(b) Inlet air temperature, 616 K (650° F).
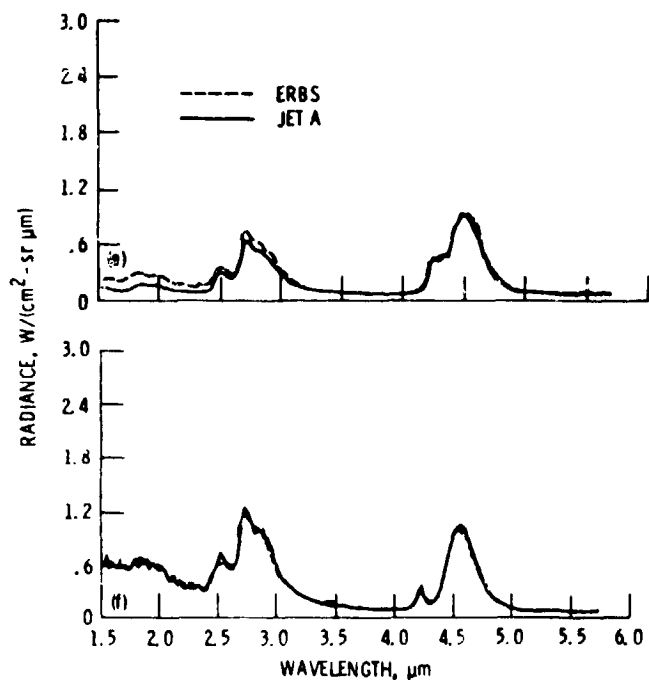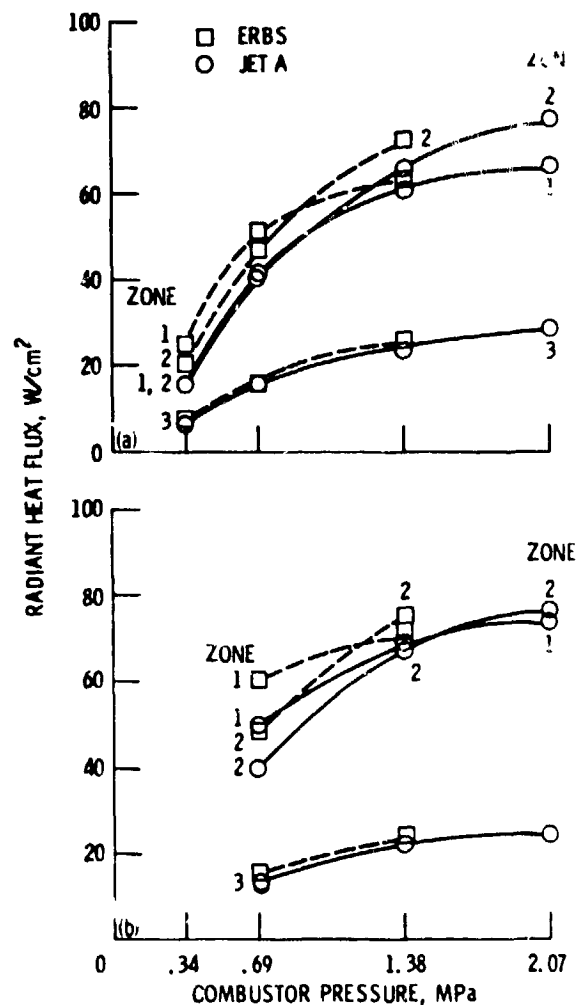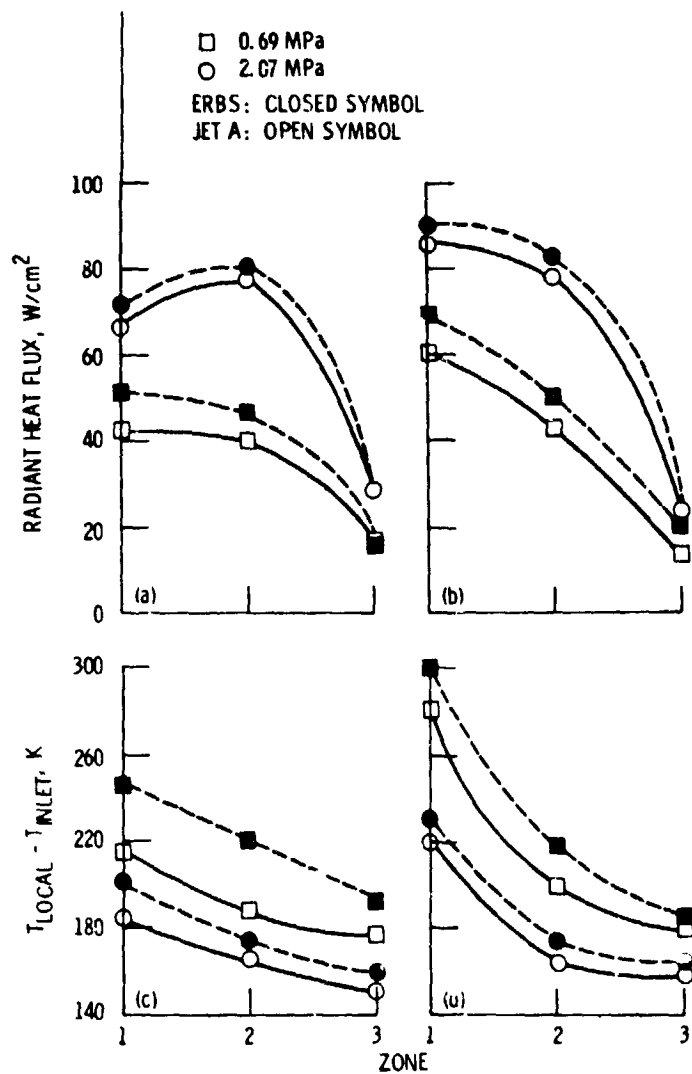
Figure 8. - Variation in total radiant heat flux by combustion zone with increase in combustor pressure; fuel-air ratio, 0.016; Jet A and ERBS fuels; fuel nozzle, FN #2.

10

Figure 9. - Comparison ui radiant heat flux variation and liner temperature variation by combustion zone; fuel-air ratio, 0.016; Jet A and ERBS fuels; combustor pressures, 0.69 MPa (100 psia) and 2.07 MPa (300 psia); fuel nozzle, FN #2.

(a) Inlet air temperature, 5⁻⁻ K (500° F).
(b) Inlet air temperature, 700 K (800° F).
(c) Inlet air temperature, 533 K (500° F).
(d) Inlet air temperature, 700 K (800° F).

11